ChemComm

COMMUNICATION

View Article Online
View Journal | View Issue

Cite this: *Chem. Commun.*, 2018, **54**, 9591

Received 28th June 2018,
Accepted 2nd August 2018

DOI: 10.1039/c8cc05193c

rsc.li/chemcomm

Pushing the limits of sensitivity and resolution for natural abundance ^{43}Ca NMR using ultra-high magnetic field (35.2 T)†

Christian Bonhomme,*[a] Xiaoling Wang,[b] Ivan Hung,[b] Zhehong Gan,[b] Christel Gervais,[a] Capucine Sassoye,[a] Jessica Rimsza,[c] Jincheng Du,[c] Mark E. Smith,[d] John V. Hanna,[e] Stéphanie Sarda,[f] Pierre Gras,[g] Christèle Combes[g] and Danielle Laurencin*[h]

Natural abundance ^{43}Ca solid state NMR experiments are reported for the first time at ultra-high magnetic field (35.2 T) on a series of Ca-(pyro)phosphate and Ca-oxalate materials, which are of biological relevance in relation to biomineralization processes and the formation of pathological calcifications. The significant gain in both sensitivity and resolution at 35.2 T leads to unprecedented insight into the structure of both crystalline and amorphous phases.

Calcium is an element of major importance, due to its abundance in living organisms and tissues (*e.g.* bone and teeth), in natural rock-forming minerals (*e.g.* francolite, calcite, and dolomite), and in major construction materials (*e.g.* cement, concrete, glass and plaster). However, determining the local environment of this element within complex molecular and materials systems is far from trivial. In particular, structural analysis by ^{43}Ca NMR spectroscopy is highly challenging, due to the poor receptivity of the NMR-active isotope.[1] Calcium-43 is indeed a spin-7/2 quadrupolar nucleus of very low natural abundance (0.14%) and resonance frequency ($\nu_0(^{43}\mathrm{Ca})$ = 57.2 MHz at B_0 = 20 T).

To tackle sensitivity issues, two main approaches have been used in the field of ^{43}Ca solid state NMR.[1–3] The first consists in analyzing large quantities of sample (typically ≥300 mg) at high magnetic field (14 to 21 T NMR instruments) under moderate magic angle spinning (MAS) conditions.[1–4] However, even when using signal enhancement NMR sequences for quadrupolar nuclei,[1,5] several hours of acquisition are needed to record a 1D spectrum, which excludes *de facto* the implementation of 2D experiments. Moreover, large quantities of material are not always available, making this approach inapplicable for many systems. The second possibility is to label in ^{43}Ca the compounds of interest.[1,5,6] However, although the gain in sensitivity allows high resolution 1D and 2D correlation experiments to be performed, the major drawback is the high cost of the isotopically-enriched precursor (~1500 € for 10 mg of 60% ^{43}Ca-labeled $CaCO_3$). Moreover, it implies that synthetic protocols often have to be re-adapted to start from ^{43}Ca-enriched $CaCO_3$ as a calcium source.

The main challenge today for ^{43}Ca solid state NMR is to find means to reach a much higher sensitivity in order to be able to perform high resolution experiments at natural abundance on a broader variety of materials. In this context, the feasibility of DNP (Dynamic Nuclear Polarization)-enhanced $\{^1\mathrm{H}\}$–^{43}Ca CP (Cross Polarization) MAS experiments at natural abundance was recently demonstrated by Lee *et al.* on a 400 MHz instrument (B_0 = 9.4 T).[7] Such DNP analyses are nevertheless constrained by specific experimental features, like the need to find efficient impregnation conditions for each material and to perform measurements at low temperatures. Moreover, the quadrupolar nature of ^{43}Ca actually calls for performing measurements at higher fields to achieve better resolution, because the second-order quadrupolar broadening scales as $1/B_0$. Hence, the possibility of recording natural abundance ^{43}Ca MAS NMR spectra at much higher magnetic fields was investigated. In this article, the first natural abundance ^{43}Ca NMR study at 35.2 T (1.5 GHz ^{1}H Larmor frequency) are reported, using the series-connected hybrid (SCH) magnet at the US National High Magnetic Field Laboratory.[8]

As the SCH magnet is available for a restricted period of time per day (~7 hours), experiments were first set up by using a ^{43}Ca-labeled monetite sample (*$CaHPO_4$). The radiofrequency (RF) power on the ^{43}Ca channel was optimized for best efficiency of the multi-DFS (double frequency sweep) signal enhancement pulse sequence (final gain in signal-to-noise: ~2).[5]

[a] *Sorbonne Université, CNRS, Collège de France, Laboratoire de Chimie de la Matière Condensée de Paris, LCMCP, F-75005 Paris, France. E-mail: christian.bonhomme@upmc.fr*
[b] *National High Magnetic Field Laboratory, 1800 East Paul Dirac Drive, Tallahassee, FL 32310-3706, USA*
[c] *Department of Materials Science and Engineering, University of North Texas, Denton, Texas 76207, USA*
[d] *Department of Chemistry, Lancaster University, Lancaster LA1 4YB, UK*
[e] *Department of Physics, Warwick University, Coventry, CV4 7AL, UK*
[f] *CIRIMAT, Université de Toulouse, CNRS, Université Paul Sabatier, 4 allée E. Monso, 31030 Toulouse cedex 4, France*
[g] *CIRIMAT, Université de Toulouse, CNRS, INPT – Ensiacet, 4 allée E. Monso, 31030 Toulouse cedex 4, France*
[h] *ICGM, UMR 5253, CNRS-UM-ENSCM, Place E. Bataillon, CC1701, 34095 Montpellier cedex 05, France. E-mail: danielle.laurencin@umontpellier.fr*

† Electronic supplementary information (ESI) available. See DOI: 10.1039/c8cc05193c

Moreover, measurements on *$CaHPO_4$ were repeated on different days using a modified/enhanced Bruker lock system, showing no detectable variation in frequency, which demonstrates the reliability of comparisons made on spectra recorded on different days. All NMR experimental parameters (including temperature, MAS probe, pulse schemes, relaxation delays, number of scans and procedure for chemical shift referencing[9]) are given in the ESI.†

Measurements on *$CaHPO_4$ illustrate the significant gain *in resolution* which is achieved at 35.2 T (Fig. 1a). Indeed, two resonances are clearly resolved at this field, and a second-order quadrupolar lineshape is even observed for the most deshielded signal, which was not the case at lower fields ($\leq$20.0 T) due to the strong overlap between resonances. The NMR parameters $\{\delta_{iso}, C_Q, \eta_Q\}$ of the two resonances were extracted by simulations at both fields. Given that the monetite structure actually exhibits 4 different Ca sites, a shifted-echo 3QMAS experiment was performed aiming at further ^{43}Ca resolution. The 2D spectrum could be recorded in just $\sim$50 minutes with a very good signal to noise ratio, due to the significant gain in sensitivity at 35.2 T (Fig. 1b). However, only two isotropic chemical shifts were observed in the f1 (indirect) dimension. According to GIPAW-DFT[10] (Gauge Including Projector Augmented Wave-Density Functional Theory) calculations on the monetite structure, this can be explained by the fact that the four inequivalent Ca sites can be divided in two groups exhibiting very similar ^{43}Ca NMR parameters, with the following averaged values:[9] $\{^{calc,avg}\delta_{iso}(^{43}Ca) = 4.2$ ppm, $^{calc,avg}C_Q(^{43}Ca) = -2.3$ MHz, $^{calc,avg}\eta_Q(^{43}Ca) = 0.40\}$ and $\{^{calc,avg}\delta_{iso}(^{43}Ca) = -4.4$ ppm $^{calc,avg}C_Q(^{43}Ca) = 1.4$ MHz, $^{calc,avg}\eta_Q(^{43}Ca) = 0.59\}$. Although this provides an explanation of the observed spectrum, understanding in detail the remaining discrepancy between these calculated average parameters and the experimental ones is still under study, and beyond the scope of the present article. Indeed, careful analyses of both the structural model of monetite and the computational approach used (including the choice of shielding reference, which is difficult to determine accurately) will need to be performed for this.

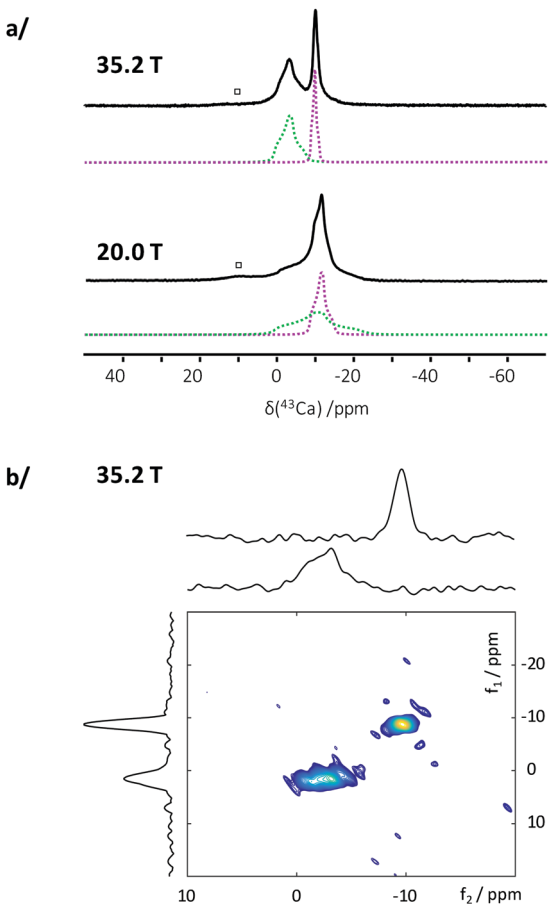

Fig. 1 (a) ^{43}Ca MAS NMR spectra of *$CaHPO_4$ at 20.0 and 35.2 T, together with their fit considering two average Ca environments $\{\delta_{iso}(^{43}Ca) = 0.7 \pm 0.8$ ppm; $|^{exp}C_Q(^{43}Ca)| = 3.5 \pm 0.3$ MHz, $^{exp}\eta_Q(^{43}Ca) = 0.8 \pm 0.1\}$, and $\{\delta_{iso}(^{43}Ca) = -8.5 \pm 0.8$ ppm; $|^{exp}C_Q(^{43}Ca)| = 1.8 \pm 0.3$ MHz, $^{exp}\eta_Q(^{43}Ca) = 0.8 \pm 0.1\}$ (□ corresponds to a minor impurity); (b) ^{43}Ca 3QMAS spectrum of *$CaHPO_4$ at 35.2 T.

With the gains in both sensitivity and resolution at 35.2 T, natural abundance ^{43}Ca MAS NMR experiments were carried out on $\sim$30 mg of crystalline calcium pyrophosphate and oxalate compounds (Fig. 2). In less than 4 hours, highly resolved spectra were obtained, while more than 5 hours and larger quantities of sample ($\sim$300 mg) had been needed previously at 20.0 T to study these phases.[2,3] Most importantly, for monoclinic calcium pyrophosphate tetrahydrate beta (m-$Ca_2P_2O_7{\cdot}4H_2O$, noted also m-CPPT β) and calcium oxalate monohydrate ($CaC_2O_4{\cdot}H_2O$, noted also COM), for which the two crystallographic Ca sites were barely resolved at 20.0 T (the isotropic chemical shifts being separated by less than 3.5 ppm),[2,3] clear resolution was achieved at 35.2 T. In contrast, for the triclinic calcium pyrophosphate dihydrate phase (t-$Ca_2P_2O_7{\cdot}2H_2O$, noted also t-CPPD), in which the ^{43}Ca isotropic shifts are separated by less than 2.5 ppm and the quadrupolar coupling constants are slightly larger ($|C_Q| \sim 3$ MHz), the two sites are not resolved. More generally, for ^{43}Ca sites characterized by $C_Q(^{43}Ca) \leq 3$ MHz, second-order quadrupolar broadening effects are almost absent at 35.2 T, and the breadth of the signals is hence a reflection of the distribution in isotropic chemical shifts and/or the intrinsic relaxation of ^{43}Ca. This is obviously the case for the COM sample (Fig. 2).

Based on the encouraging measurements made on the crystalline Ca-pyrophosphate and oxalate phases (Fig. 2), the characterization of an amorphous pyrophosphate phase $Ca_2P_2O_7{\cdot}xH_2O$ (a-CPP, $x \sim 4$) at 35.2 T was undertaken. This sample represented a much greater challenge for natural abundance ^{43}Ca NMR, due to wider range of variation of the chemical shift and quadrupolar NMR parameters, which lead to broader signals.[2] Moreover, given that Ca-sites with large quadrupolar coupling constants ($|C_Q(^{43}Ca)| > 5.5$ MHz) may be found in amorphous materials,[11] natural abundance ^{43}Ca MAS NMR measurements at "lower" fields ($B_0 \leq 20$ T) using spinning speeds of $\sim$5 kHz (which is in practice the upper limit for some of the commercial large volume rotors) could actually lead to misleading lineshapes. As a matter of fact, very few data related to calcium-containing glasses (labeled in ^{43}Ca),[12,13] and amorphous derivatives (in natural abundance) have been published so far.[1,2]

The natural abundance ^{43}Ca MAS NMR spectrum of a-CPP was recorded at 35.2 T (Fig. 3a). Thanks to the very fast relaxation

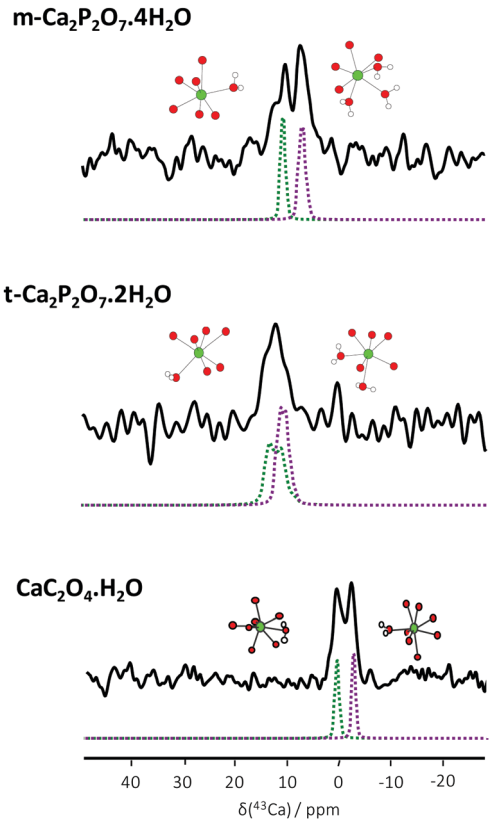

Fig. 2 Natural abundance ^{43}Ca MAS NMR spectra of m-$Ca_2P_2O_7{\cdot}4H_2O$ (m-CPPT β, 2.5 hours), t-$Ca_2P_2O_7{\cdot}2H_2O$ (t-CPPD, 3 hours) and $CaC_2O_4{\cdot}H_2O$ (COM, 3 hours), recorded at 35.2 T. The dashed lines show the simulation of the contributions of the two inequivalent Ca-sites in each structure, using the experimental ^{43}Ca NMR parameters determined previously (which are recalled in ESI† in Table S2).[2,3]

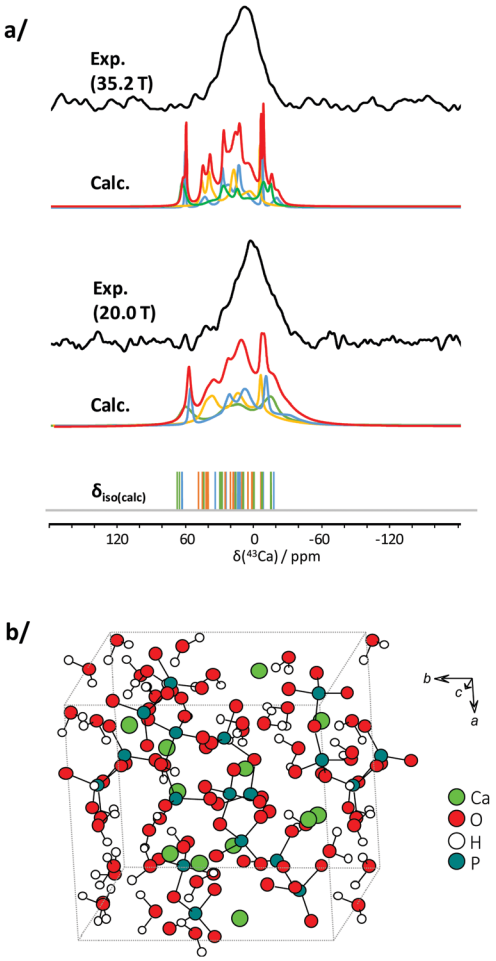

Fig. 3 (a) ^{43}Ca MAS NMR spectra of amorphous-$Ca_2P_2O_7{\cdot}4H_2O$ (a-CPP) at 20.0 and 35.2 T, together with the GIPAW-DFT ^{43}Ca NMR calculations related to the three AIMD derived models (sum in red, contributions of models I, II and III in blue, orange and green respectively; calculated isotropic shifts are shown as vertical bars); (b) AIMD derived computational model of a-CPP (model I) used for DFT calculations (see ESI† for further details as each of three models provides 12 calcium sites).

of ^{43}Ca in the sample, less than 4 hours were needed to record the spectrum, which is all the more remarkable when considering that the signal is ~10 times broader in comparison to those of the crystalline phases reported above.

In order to gain greater 'chemical insight' into the origin of these distributions, computational models of the amorphous compound were developed, using Monte Carlo (MC) based simulations with bond constraints followed by relaxation with *Ab Initio* Molecular Dynamics (AIMD) simulations and geometry optimization with DFT calculations (see ESI†). It should be noted that in contrast to non-hydrated calcium derived glasses,[13] the commonly used melt-quench approach for MD could not be used to model amorphous $Ca_2P_2O_7{\cdot}4H_2O$, as it would have led to condensed phosphate chains with various lengths and would not have been able to tackle the presence of water molecules. Here, using combined MC, AIMD, and DFT calculations, three models of this amorphous phase with hydrated calcium pyrophosphate groups were generated (each with 12 Ca sites, see Fig. 3b).‡ For each model, calculated Pair Distribution Function (PDF) analyses were compared to the experimental data, showing that the agreement is reasonable (Fig. S3 in ESI†).

The analysis of the Ca local environments in these models demonstrates that (i) coordination numbers range between 4 and 9, (ii) up to 5 water molecules can be bound to Ca^{2+}, and (iii) the average Ca···O bond distances are between 2.3 and 2.6 Å (see ESI,† Table S4). These values are in agreement with the structural parameters of the crystalline calcium pyrophosphate phases (dihydrate and tetrahydrate). Coordination numbers range from 6 to 7 for calcium atoms in these structures and bond distances are between 2.257 and 2.668 Å.[14–16] DFT calculations of the ^{43}Ca NMR parameters were then carried out, using the GIPAW-DFT approach (see ESI† for computational details). The range of variation of the calculated isotropic chemical shift (-16.1 ppm $< {}^{calc}\delta_{iso}(^{43}Ca) <$ 64.3 ppm; average value of 21.6 ppm) and quadrupolar coupling constants (1.2 MHz $< |{}^{calc}C_Q(^{43}Ca)| <$ 6.5 MHz; average value of 3.4 MHz) is consistent with the experimental data (Fig. 3a). More specifically, it is worth noting that the calculated values ${}^{calc}\delta_{iso}(^{43}Ca)$ spread out across the experimental lineshape obtained at 35.2 T, with more of the calculated values positioned towards where the signal has maximum intensity. Despite the lack of sufficient statistics at

this stage, which are visible from the simulated sums of the models (Fig. 3a, red curves), these AIMD models appear as the first realistic starting point for describing Ca local environments in these amorphous materials. In Fig. S4 (ESI†), additional simulations including Czjzek distributions of quadrupolar parameters (Gaussian Isotropic Model, GIM) as well as Gaussian distributions of ^{43}Ca isotropic chemical shifts[17] are presented, which show that at ultra-high magnetic field, it is likely that simple distributions of isotropic chemical shifts are mainly observed. Finally, it should be noted that GIPAW NMR calculations were performed at 0 K, therefore not taking into account potential local dynamics of the water molecules,[2] which could affect the ^{43}Ca NMR parameters. Low temperature ^{43}Ca NMR experiments will need to be performed in the future to investigate this aspect.

All in all, the 1.5 GHz series connected hybrid instrument paves new avenues for natural abundance ^{43}Ca MAS NMR. Significant gains in both resolution and sensitivity were demonstrated in the case of crystalline calcium pyrophosphate and oxalate phases. Most importantly, thanks to favorable relaxation characteristics, the natural abundance ^{43}Ca MAS NMR spectrum of an amorphous hydrated calcium pyrophosphate was successfully obtained, which could be compared for the first time to models generated by AIMD computer simulations of this phase. This point is of crucial importance as amorphous precursors of calcium carbonate,[18] calcium oxalate[19] and calcium (pyro)phosphates[20] are meant to play a fundamental role in biomineralization processes, which have not been fully characterized so far (notably regarding Ca environments). Moreover, such ^{43}Ca NMR experiments at ultra-high magnetic field may also provide complementary clues regarding the polyamorphism of biomaterials.[2,21]

The French National Research Agency (ANR) is acknowledged for financial support (“CAPYROSIS” project – ANR-12-BS08-0022-01; “PYVERRES” project – ANR-16-CE19-0013). A portion of this work was performed at the National High Magnetic Field Laboratory, which is supported by the National Science Foundation Cooperative Agreement No. DMR-1157490 & DMR-1644779, and the State of Florida. JD acknowledges financial support of National Science Foundation (NSF) Ceramics Program DMR-1508001. The UK 850 MHz solid-state NMR Facility used in this research was funded by EPSRC and BBSRC (contract PR140003), as well as the University of Warwick including part funding through Birmingham Science City Advanced Materials Projects 1 and 2 supported by Advantage West Midlands (AWM) and the European Regional Development Fund (ERDF). NMR spectroscopic calculations were performed using HPC resources from GENCI-IDRIS (Grant 097535).

Conflicts of interest

There are no conflicts to declare.

Notes and references

‡ Due to the high computational cost of the AIMD simulations (see ESI† for further details), only 3 models of the a-CPP phase have been generated so far, with a general formula $Ca_2P_2O_7{\cdot}4H_2O$. It should be noted that in the amorphous phases characterized experimentally, the pyrophosphate content is slightly lower ($\sim$3.5–3.9 H_2O per pyrophosphate).

1 C. M. Widdifield, *Annu. Rep. NMR Spectrosc.*, 2017, **92**, 227; D. Laurencin and M. E. Smith, *Prog. Nucl. Magn. Reson. Spectrosc.*, 2013, **68**, 1; D. Bryce, *Dalton Trans.*, 2010, **39**, 8593.
2 P. Gras, A. Baker, C. Combes, C. Rey, S. Sarda, A. J. Wright, M. E. Smith, J. V. Hanna, C. Gervais, D. Laurencin and C. Bonhomme, *Acta Biomater.*, 2016, **31**, 348.
3 H. Colas, L. Bonhomme-Coury, C. Coelho Diogo, F. Tielens, F. Babonneau, C. Gervais, D. Bazin, D. Laurencin, M. E. Smith, J. V. Hanna, M. Daudon and C. Bonhomme, *CrystEngComm*, 2013, **15**, 8840.
4 S. Chen, B. E. G. Lucier, M. Chen, V. V. Terskikh and Y. Huang, *Chem. – Eur. J.*, 2018, **24**, 8732.
5 K. M. N. Burgess, F. A. Perras, I. L. Moudrakovski, Y. Xu and D. L. Bryce, *Can. J. Chem.*, 2015, **93**, 799.
6 D. Laurencin, A. Wong, J. V. Hanna, R. Dupree and M. E. Smith, *J. Am. Chem. Soc.*, 2008, **130**, 2412; A. Wong, D. Laurencin, R. Dupree and M. E. Smith, *Solid State Nucl. Magn. Reson.*, 2009, **35**, 32; D. Laurencin, C. Gervais, A. Wong, C. Coelho, F. Mauri, D. Massiot, M. E. Smith and C. Bonhomme, *J. Am. Chem. Soc.*, 2009, **131**, 13430.
7 D. Lee, C. Leroy, C. Crevant, L. Bonhomme-Coury, F. Babonneau, D. Laurencin, C. Bonhomme and G. De Paëpe, *Nat. Commun.*, 2017, **8**, 14104.
8 Z. Gan, I. Hung, X. L. Wang, J. Paulino, G. Wu, I. M. Litvak, P. L. Gor'kov, W. W. Brey, P. Lendi, J. L. Schiano, M. D. Bird, L. R. Dixon, J. Toth, G. S. Boebinger and T. A. Cross, *J. Magn. Reson.*, 2017, **284**, 125.
9 C. Gervais, D. Laurencin, A. Wong, F. Pourpoint, J. Labram, B. Woodward, A. P. Howes, K. J. Pike, R. Dupree, F. Mauri, C. Bonhomme and M. E. Smith, *Chem. Phys. Lett.*, 2008, **464**, 42.
10 C. J. Pickard and F. Mauri, *Phys. Rev. B: Condens. Matter Mater. Phys.*, 2001, **63**, 245101.
11 A. Pedone, T. Charpentier and M. C. Menziania, *Phys. Chem. Chem. Phys.*, 2010, **12**, 6054.
12 K. Shimoda, Y. Tobu, Y. Shimoikeda, T. Nemoto and K. Saito, *J. Magn. Reson.*, 2007, **186**, 156; F. Angeli, M. Gaillard, P. Jollivet and T. Charpentier, *Chem. Phys. Lett.*, 2007, **440**, 324.
13 E. Gambuzzi, A. Pedone, M. C. Menziani, F. Angeli, P. Florian and T. Charpentier, *Solid State Nucl. Magn. Reson.*, 2015, **68–69**, 31.
14 N. S. Mandel, *Acta Crystallogr., Sect. B: Struct. Crystallogr. Cryst. Chem.*, 1975, **31**, 1730.
15 T. Balić-Žunić, M. R. Christoffersen and J. Christoffersen, *Acta Crystallogr., Sect. B: Struct. Sci.*, 2000, **56**, 953.
16 P. Gras, C. Rey, G. André, C. Charvillat, S. Sarda and C. Combes, *Acta Crystallogr., Sect. B: Struct. Sci., Cryst. Eng. Mater.*, 2016, **72**, 96.
17 D. R. Neuville, L. Cormier and D. Massiot, *Geochim. Cosmochim. Acta*, 2004, **68**, 5071.
18 Y. Wang, S. Von Euw, F. M. Fernandes, S. Cassaignon, M. Selmane, G. Laurent, G. Pehau-Arnaudet, C. Coelho, L. Bonhomme-Coury, M.-M. Giraud-Guille, F. Babonneau, T. Azaïs and N. Nassif, *Nat. Mater.*, 2013, **12**, 1144; S. Weiner, Y. Levi-Kalisman, S. Raz and L. Addadi, *Connect. Tissue Res.*, 2003, **44**, 24.
19 E. Ruiz-Agudo, A. Burgos-Cara, C. Ruiz-Agudo, A. Ibanez-Velasco, H. Cölfen and C. Rodriguez-Navarro, *Nat. Commun.*, 2017, **8**, 768.
20 K. Ley-Ngardigal, C. Combes, S. Teychene, C. Bonhomme, C. Coelho-Diogo, P. Gras, C. Rey and B. Biscans, *Cryst. Growth Des.*, 2017, **17**, 37.
21 J. H. E. Cartwright, A. G. Checa, J. D. Gale, D. Gebauer and C. I. Sainz-Diaz, *Angew. Chem.*, 2012, **51**, 11960.

